

Single-domain versus two-domain configuration in thin ferromagnetic prisms

Maria Gloria Pini, Paolo Politi

Istituto dei Sistemi Complessi, Consiglio Nazionale delle Ricerche, Via Madonna del Piano 10, 50019 Sesto Fiorentino, Italy

Abstract

Thin ferromagnetic elements in the form of rectangular prisms are theoretically investigated in order to study the transition from single-domain to two-domain state, with changing the in-plane aspect ratio p . We address two main questions: first, how general is the transition; second, how the critical value p_c depends on the physical parameters. We use two complementary methods: discrete-lattice calculations and a micromagnetic continuum approach. Ultrathin films do not appear to split in two domains. Instead, thicker films may undergo the above transition. We have used the continuum approach to analyze recent Magnetic Force Microscopy observations in 30nm-thick patterned Permalloy elements, finding a good agreement for p_c .

Key words: Magnetic nanostructures, Magnetic domains, Permalloy

PACS: 75.75.+a, 75.60.Ch, 75.10.-b

1 Introduction

In recent years, arrays of patterned ferromagnetic dots have received considerable interest owing to their possible applications in high-density magnetic data storage [1] and spin-electronic [2] devices, as well as for realizing logic functionality [3]. High-resolution electron beam lithographic techniques [4] are commonly used to fabricate the samples, in such a way that all the particles in the array are virtually identical to each other. As a consequence, the measured properties of the array can be interpreted as the individual properties of a single dot, provided that the dots are sufficiently far spaced to neglect the interdot magnetostatic interaction. In this way, using high-sensitivity magneto-optical

Email addresses: mariagloria.pini@isc.cnr.it (Maria Gloria Pini), paolo.politi@isc.cnr.it (Paolo Politi).

magnetometry techniques, the variation of the properties with the shape in magnetic nanoelements could be experimentally investigated for dots as thin as 3 nm [5]. Single dot properties can also be investigated by magnetic force microscopy (MFM) techniques [6], which allow to focus on a single element.

In this paper, we will consider in-plane magnetized dots [1]. Within the plane, the preferred direction of the magnetization is determined by a balance between magnetic dipole-dipole interaction and magnetocrystalline anisotropy [7]. In Permalloy elongated nanodots, the direction of the uniform magnetization is determined by the shape-induced magnetic anisotropy, since the crystalline anisotropy of the material is negligible.

In a recent paper [8] we studied rectangular monolayers of planar spins located on the sites of a two-dimensional triangular lattice and interacting via magnetic dipole-dipole interaction only. For this lattice geometry, the infinite monolayer (ML) is believed [9] to have a ferromagnetic (FM) ground state, which is degenerate with the orientation. The infinite square lattice is instead believed to have a microvortex ground state, which is degenerate with a local orientation angle. For specific values of this angle, we get a state of FM lines antiferromagnetically coupled. Therefore, the difference between the two types of lattice is often understood in terms of the coupling between FM lines of spins, which is ferromagnetic in the triangular lattice and antiferromagnetic in the square lattice.

In our paper [8], rectangular monolayers were studied with varying their size and aspect ratio p , defined as the ratio between the smaller and the larger side of the rectangle.¹ Two main results came out. First, passing from rectangular, elongated finite systems to square-shaped ones, we obtained clear evidence for a transition from a FM to a two-domain and eventually to a macrovortex state configuration. Second, in the thermodynamic limit, we found that the macrovortex seems to be the lowest energy state whatever is the aspect ratio, but for elongated samples the size must attain unphysically large values to display such a state.

In this paper, we want to study the effect of a direct exchange interaction between spins, taking into account the effect of a variable thickness as well. These generalizations make our result relevant for FM prisms which are currently available. A recent paper [11] by Jubert and Allenspach moved along similar lines, with the authors studying the transition from single-domain to macrovortex configuration for a circular ferromagnetic disk. Here, we are rather interested in the problem of the transition from single-domain to two-

¹ Such a definition was adopted here for better convenience as regards the comparison with the experimental data in Ref. [3]. Note that it differs both from the one adopted by Aharoni in Ref. [10] and from the one we used in Ref. [8] ($r = 1/p$ rather than p).

domain configuration. For this reason, we study a thin rectangular ferromagnetic prism.

We want to address two main questions:

i) How general is the transition? We have already shown [8] that this transition occurs for a purely dipolar system in the ML limit. Introducing the exchange coupling, A , makes the domain wall more energetically expensive and change the width of the domain wall: the latter is atomically sharp for a purely dipolar system, while it spreads over many lattice constants when $A \neq 0$. Here, we want to ascertain whether these changes are able to cancel the transition and whether lattice structure effects, which are so important for a purely dipolar system, are maintained.

ii) If a transition occurs, how does the critical value, p_c , of the in-plane aspect ratio, p , of the rectangular element depend on the physical parameters of the system?

We will use two complementary methods for the evaluation of the magnetostatic energy difference, ΔE_M , between a two-domain state and a single-domain state: discrete-lattice calculations, which are valid for ultrathin films, and a micromagnetic continuum approach, applicable to thicker films.

In Section II discrete-lattice calculations are performed for a rectangular monolayer, both for spins located on a triangular and on a square lattice. Our main result is that the transition from a single-domain state to a two-domain state is suppressed, in the ultrathin limit, because of the exchange-induced broadening of the domain wall, which modifies the energetic balance of the dipolar energy. This result does not depend on the type of lattice, because spin configurations varying on scales much larger than the lattice constant depend weakly on lattice geometry.

In the case of thicker samples, a micromagnetic approach is appropriate. In Section III we calculate the magnetostatic energy difference, ΔE_M , between the two-domain and the single-domain state, following a method devised a few years ago by Aharoni [10]. In the limit of domain-wall width much smaller than the lateral dimensions of the ferromagnetic dot, analytical expressions can be obtained both for the magnetostatic energy gain, ΔE_M , due to *surface* charges and for the energy cost (per unit wall area), γ_N , of a one dimensional Néel wall [12,13]. For a thin rectangular prism, γ_N includes contributions from the exchange interaction, the uniaxial magnetocrystalline anisotropy, and the magnetostatic energy due to *volume* charges in the Néel wall. One can thus estimate in a simple way the critical value, p_c , of the in-plane aspect ratio separating the single-domain phase from the two-domain phase.

An important remark is in order here. Introducing the exchange interaction,

A , has a twofold effect: i) the domain wall width is increased to a value $L_{dw} \approx \sqrt{A/K_1}$, where K_1 is the uniaxial anisotropy constant, and ii) the domain wall energy density (*i.e.*, the energy per unit wall area) is increased by a quantity of order $\sqrt{AK_1}$. A two-domain state can be energetically favorable if the gain in dipolar energy density coming from the two opposite domains, of order $M_s^2 b$ (where M_s is the saturation magnetization and $2b$ is the thickness), prevails on the full domain wall energy density, which has a dipolar contribution plus the just mentioned term of order $\sqrt{AK_1}$. A necessary condition for the transition to occur is that the two-domain configuration is energetically favorable when $A = 0$, because the exchange (and the anisotropy) only contribute to the cost of the energy balance, *not* to the gain. If the transition does occur when $A = 0$, one can wonder whether the transition is maintained when $A \neq 0$. One is thus led to conclude that, for comparable values of the anisotropy and dipolar energy densities ($K_1 \approx M_s^2$), the transition disappears because the domain wall energy density (of order $\sqrt{AK_1}$) surely dominates on the gain (of order $M_s^2 d$). Such a no-domain rule for in-plane configurations in ultrathin films had already been found in Refs. [7,14].

However, there are systems where K_1 is so small that the term $\sqrt{AK_1}$ is comparable to, or even smaller than, $M_s^2 b$: this is just the case of Permalloy. In fact, our theoretical predictions about the occurrence of a transition from a single-domain to a two-domain state in rectangular Permalloy dots when increasing the in-plane aspect ratio p are confirmed by recent MFM data [3] of *elliptic* patterned Permalloy elements with thickness 30 nm, lateral size 3 μm and p varying between the values $p = 0.13$ (elongated dot, single-domain state) and $p \lesssim 1$ (almost circular dot, two-domain state).

Finally, in Section 4 we compare the discrete and the continuum approaches. There are some indications that the transition from single-domain to two-domain state may appear when the thickness of the film is comparable to the width of the domain wall. Final considerations are reported in Section 5.

2 Discrete-lattice calculation of the magnetic dipolar energy of a one-monolayer-thick rectangular element

Let us start considering a rectangular element which is one monolayer thick. We want to compare the energy of the in-plane ferromagnetic (FM) configuration, where all spins (because of shape anisotropy) are parallel to the longer side, to the two-domain configuration (see Fig. 1), where a single Néel domain wall, parallel to the longer side, is inserted in the middle of the stripe. We have considered both a triangular and a square lattice, with the \hat{z} axis parallel to a row of atoms. However, for ease of notations, we will refer to the square lattice. Different rows are labelled with index m as follows: for

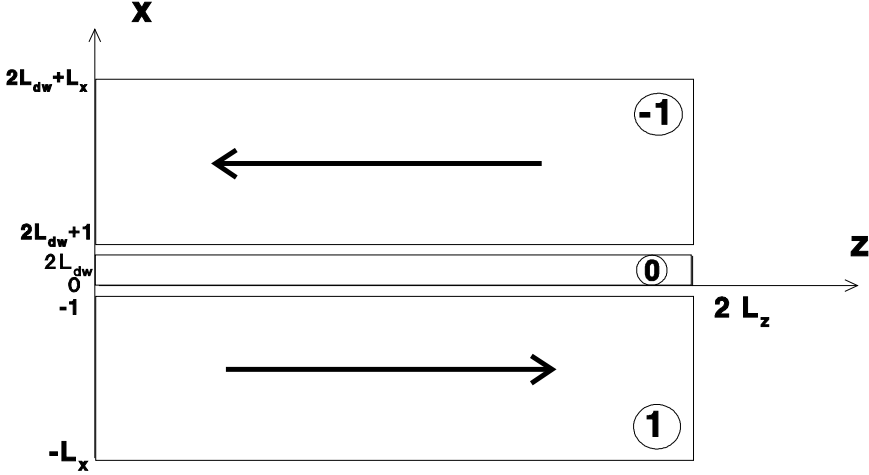


Fig. 1. The geometry of the rectangular element in the two-domain configuration. The bold arrows denote the magnetization directions and $2L_{dw}$ is the domain wall width.

$-L_x \leq m \leq -1$ (region ‘1’), the spins are parallel to the $+\hat{z}$ direction, $\vec{S} = \hat{z}$; when m varies between $m = 0$ and $m = 2L_{dw}$ (region ‘0’), the spins rotate inside the domain wall, according to the relations $S_x(m) = \cos[m\pi/(2L_{dw})]$ and $S_y(m) = \sin[m\pi/(2L_{dw})]$; finally, for $2L_{dw} + 1 \leq m \leq 2L_{dw} + L_x$ (region ‘-1’), $\vec{S} = -\hat{z}$. If the distance between nearest neighboring spins is taken as length unit, the size of the stripe in the \hat{z} direction is $2L_z$ and lines parallel to \hat{z} are distant 1.

The full dipolar energy of a given configuration can be written as

$$E_{dip} = \Omega \sum_{(ij)} \frac{1}{r_{ij}^3} \left[\vec{S}_i \cdot \vec{S}_j - 3 \frac{(\vec{S}_i \cdot \vec{r}_{ij})(\vec{S}_j \cdot \vec{r}_{ij})}{r_{ij}^2} \right], \quad (1)$$

where $\Omega = \mu^2/a_0^3 = M_s^2 a_0^3$ (μ is the magnetic moment per spin, M_s is the magnetic moment per unit volume, and a_0 is the lattice constant).

Interacting spins (ij) can be grouped according to the regions, ‘1’, ‘0’ and ‘-1’, they belong to, so that:

$$E_{dip} = E_{1,1} + E_{0,0} + E_{-1,-1} + E_{1,0} + E_{-1,0} + E_{1,-1}. \quad (2)$$

The first three terms are the self-energies of the three regions; $E_{1,0}$ and $E_{-1,0}$ are the interaction energies between each ferromagnetic region and the domain wall region; finally, $E_{1,-1}$ is the energy between the two ferromagnetic regions. We are interested in the energy difference between the two-domain state and the FM (single-domain) state. Since it will be useful to consider ener-

gies per unit length in the \hat{z} direction, we define $\Delta E_{dip} = (E_{dip} - E_{dip}^{FM})/(2L_z)$, where E_{dip} and E_{dip}^{FM} are the energies of the two-domain and of the FM state, respectively. When the symbols E and E^{FM} are accompanied by the subscripts ‘1’, ‘0’, ‘-1’, the energies refer to self/interaction dipolar energies of specific regions. Since regions ‘1’ and ‘-1’ keep themselves ferromagnetic, $\Delta E_{1,1} = \Delta E_{-1,-1} = 0$, and

$$\Delta E_{dip} = \Delta E_{0,0} + \Delta E_{1,0} + \Delta E_{-1,0} + \Delta E_{1,-1}. \quad (3)$$

As for $\Delta E_{1,0}$ and $\Delta E_{-1,0}$ (which are equal, for symmetry reasons), they can be neglected [15,16], because the interaction between a FM domain and the domain wall is averaged to zero in the limit $L_x \gg L_{dw}$. Finally, we have

$$\Delta E \simeq \Delta E_{0,0} + \Delta E_{1,-1}, \quad (4)$$

where the first term is the self-energy of the domain wall and the second term is the interaction energy between the two FM regions. In Fig. 2 (main) we show that $\Delta E_{0,0}$ goes to a constant with increasing L_z , so that we can define a dipolar domain wall energy per unit length. As for the L_{dw} -dependence of $\Delta E_{0,0}$, it is shown in the inset of the same figure. For a large range of values of L_{dw} , $1 \ll L_{dw} \ll L_z$, $\Delta E_{0,0}$ can be approximately taken as constant. In conclusion, we can assume that $\Delta E_{0,0}/\Omega$ is a constant d_0 , with $d_0 \simeq 4$.

The quantity $\Delta E_{1,-1}$ can be rewritten as follows,

$$\Delta E_{1,-1} = (E_{1,-1} - E_{1,-1}^{FM})/(2L_z) = -2E_{1,-1}^{FM}/(2L_z), \quad (5)$$

because in the two-domain state, the spins in the ‘-1’ region are just reversed with respect to the FM state. Since the two regions are $2L_{dw}$ far away, we can replace the discrete summation by an integral. We get the result:

$$\begin{aligned} E_{1,-1}^{FM}/\Omega = & 2\sqrt{4L_z^2 + 2L_{dw}^2} - 4\sqrt{4L_z^2 + (L_x + 2L_{dw})^2} + 2\sqrt{4L_z^2 + (2L_x + 2L_{dw})^2} \\ & - 4(L_x + 2L_{dw}) \ln(L_x + 2L_{dw}) + 2L_{dw} \ln 2L_{dw} \\ & - (6L_x + 8L_{dw}) \ln[\sqrt{4L_z^2 + (L_x + 2L_{dw})^2} - L_x - 2L_{dw}] \\ & - 2L_x \ln[\sqrt{4L_z^2 + (L_x + 2L_{dw})^2} + L_x + 2L_{dw}] \\ & + 2(2L_x + 2L_{dw}) \ln(2L_x + 2L_{dw}) + 2(L_x + 2L_{dw}) \ln[\sqrt{4L_z^2 + 2L_{dw}^2} - 2L_{dw}] \\ & + 2L_x \ln[\sqrt{4L_z^2 + 2L_{dw}^2} + 2L_{dw}] \\ & + 2(2L_x + 2L_{dw}) \ln[\sqrt{4L_z^2 + (2L_x + 2L_{dw})^2} - 2L_x - 2L_{dw}]. \end{aligned} \quad (6)$$

In the relevant limit $L_{dw} \ll L_z, L_x$, we get

$$\Delta E_{1,-1}/\Omega \simeq -4 \left\{ 1 + p \ln 4 - \sqrt{4+p^2} + \sqrt{1+p^2} - p \ln \left(\frac{\sqrt{4+p^2}-p}{\sqrt{1+p^2}-p} \right) \right\}, \quad (7)$$

where $p = L_x/L_z$ is the aspect ratio of the stripe. The above function, which gives the gain in dipolar energy from the interaction of the two FM regions with opposite magnetization, varies between $\Delta E_{1,-1} = 0$ for $p = 0$ (infinitely elongated sample) to $\Delta E_{1,-1} \simeq -1.9\Omega$ for $p = 1$ (square sample).

The two-domain state can be favored with respect to the FM state only if $\Delta E_{dip} \simeq \Delta E_{0,0} + \Delta E_{1,-1} < 0$. Since $\Delta E_{0,0} \approx 4\Omega$ and $\Delta E_{1,-1} \approx -2\Omega$, the conclusion is that a two-domain state with an *extended* domain wall can *not* appear in a one-monolayer thick stripe, whatever the aspect ratio is. For the triangular lattice one has $\Delta E_{0,0} \approx 5\Omega$ and $\Delta E_{1,-1} \approx -2\Omega$, so the same conclusion can be drawn. This is not in contradiction with what we found in Ref. [8], because there we assumed an atomically *sharp* domain wall ($L_{dw} = 0$ in the present notations).

As stressed in the Introduction, the reason why we are now considering $L_{dw} \gg 1$, is because exchange interaction widens the domain wall. It is well known [13] that in the presence of a short range ferromagnetic interaction, A , and of a uniaxial anisotropy, K_1 (favoring the $\pm\hat{z}$ directions), the additional contribution to the domain wall energy per unit length is $\Delta E_{ex+ani} \approx \sqrt{AK_1} > 0$ and the resulting domain wall width is $L_{dw} \approx \sqrt{A/K_1}$. Therefore, the total energy difference (per unit length) ΔE_{total} between the two-domain and the FM single domain state is

$$\Delta E_{total} = \Delta E_{0,0} + \Delta E_{1,-1} + \Delta E_{ex+ani}. \quad (8)$$

Since the gain in energy of a two-domain state must be provided by dipolar energy, a positive value for $(\Delta E_{0,0} + \Delta E_{1,-1})$ can *not* be healed by the additional positive term ΔE_{ex+ani} . The conclusion of this Section is that a single FM monolayer does not split into two domains if exchange interaction makes the domain wall width finite.

3 Micromagnetic calculation of the magnetostatic energy of a rectangular prism

A few years ago, Aharoni [10] gave an analytic expression for the demagnetizing factors of a uniform and homogeneous ferromagnetic particle in the shape of a rectangular prism, extending over the volume $-a \leq x \leq a$, $-b \leq y \leq b$

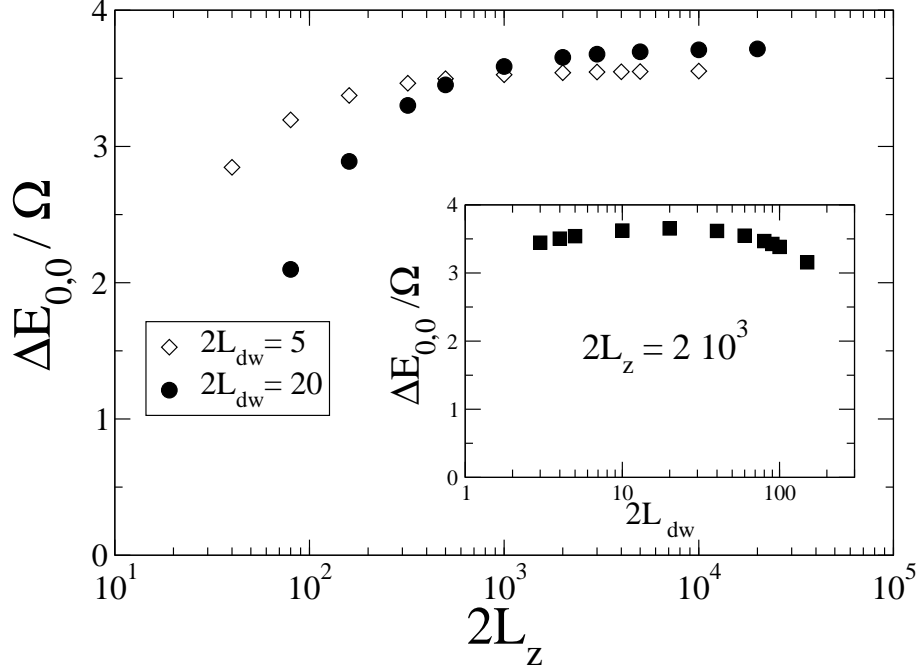


Fig. 2. Main: The dipolar contribution to the domain wall energy per unit length, $\Delta E_{0,0}$, as a function of $2L_z$, for $2L_{dw} = 5$ (circles) and $2L_{dw} = 20$ (diamonds). Inset: The same quantity, $\Delta E_{0,0}$, as a function of L_{dw} , for $L_z = 10^3$. All results refer to a square lattice.

and $-c \leq z \leq c$, with the origin of the Cartesian coordinate system at the center of the prism (see Fig. 3, top). With respect to the notations used in the previous Section, we have $a = a_0 L_x$, $b = a_0 L_y$, $c = a_0 L_z$, and $w = a_0 L_{dw}$ (see footnote²). Here we briefly sketch Aharoni's calculation [10] for clarity's sake.

When the prism is saturated along $+z$, surface charges $\pm M_s$ are created on the faces $z = \pm c$, where M_s is the saturation magnetization. The potential due to the surface charges is (in cgs units) [13]

$$U(\mathbf{r}) = \int_S \frac{\mathbf{n} \cdot \mathbf{M}(\mathbf{r}')}{|\mathbf{r} - \mathbf{r}'|} dS'. \quad (9)$$

The density of the surface charges is $(\mathbf{n} \cdot \mathbf{M})$ where \mathbf{M} is the magnetization and \mathbf{n} , the unit normal to the surface S of the ferromagnetic body, is taken to be positive in the outward direction. The magnetic field generated by the surface charge distribution is $\mathbf{H} = -\nabla U$ and the magnetostatic self-energy is

² Since $L_{dw} \ll L_x$, the definitions $a = a_0 L_x$ and $a = a_0(L_x + L_{dw})$ are equivalent.

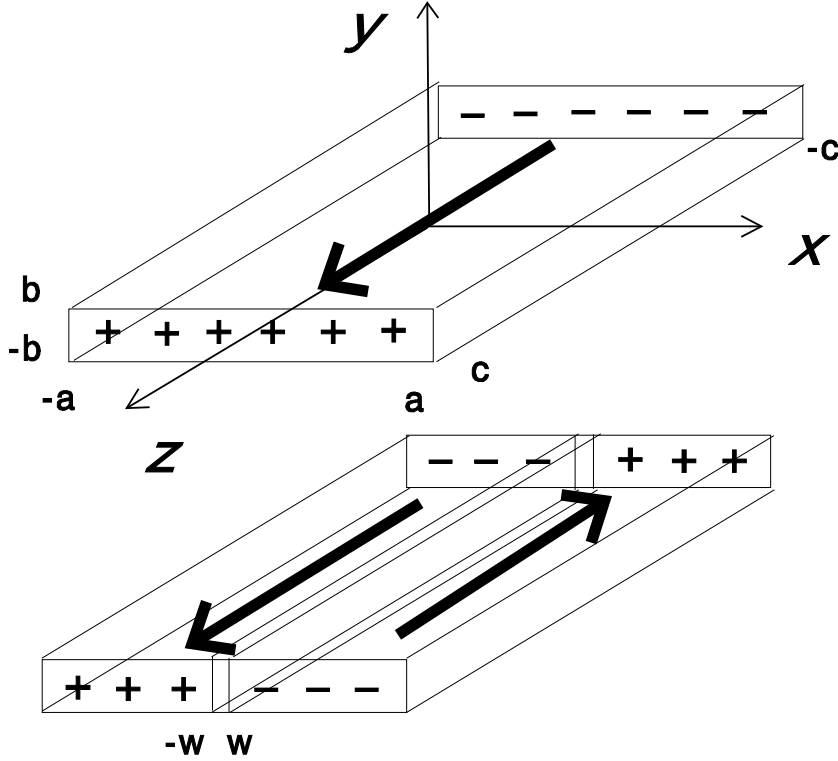


Fig. 3. The geometry of the rectangular ferromagnetic prism. The bold arrows denote the magnetization directions. Schematic representations of the surface magneto-static charges are displayed for the single-domain state (top) and for the two-domain state (bottom).

given by

$$E_M = -\frac{1}{2} \int_V \mathbf{M} \cdot \mathbf{H} dV', \quad (10)$$

where the integration is over the volume V of the ferromagnetic body. As a general rule [13,17], it is not advisable to evaluate first the potential U for a specific case, then obtain the magnetostatic field $\mathbf{H} = -\nabla U$, and finally substitute \mathbf{H} in Eq. (10). It is better to write (10) with all its integrals and then consider which to perform first. In other words, the order in which integrations are carried can considerably change the amount of algebra. The magnetostatic self-energy of the uniform rectangular prism depicted in Fig. 3 (top) is

$$E_M^{\uparrow\uparrow} = \frac{1}{2} M_s^2 \int_{-c}^{+c} dz \frac{\partial}{\partial z} \int_{-b}^b dy \int_{-b}^b d\eta \int_{-a}^a dx \int_{-a}^a d\xi$$

$$\left[\frac{1}{\sqrt{(x-\xi)^2 + (y-\eta)^2 + (z-c)^2}} - \frac{1}{\sqrt{(x-\xi)^2 + (y-\eta)^2 + (z+c)^2}} \right].$$

By carrying out analytically the four integrations over x, y, ξ, η (see Appendix A for details) one obtains

$$E_M^{\uparrow\uparrow} = \frac{1}{2} M_s^2 V N_z, \quad (11)$$

where the explicit expression for N_z , the demagnetizing factor of the general rectangular prism of volume $V = 8abc$, is given in Ref. [10]. In general one has $N_x + N_y + N_z = 4\pi$; for a cubic sample ($a = b = c$), $N_x = N_y = N_z = \frac{4\pi}{3}$.

When the rectangular prism is divided into two domains with opposite magnetizations directed along $\pm z$ (see Fig. 3, bottom), the contribution of surface charges to the magnetostatic energy is

$$E_M^{\downarrow\uparrow} = \frac{1}{2} M_s^2 \left\{ \int_{-c}^{+c} dz \frac{\partial}{\partial z} \int_{-b}^b dy \int_{-b}^b d\eta \int_{-a}^a dx \int_{-a}^{-w} d\xi \left[\frac{1}{\sqrt{(x-\xi)^2 + (y-\eta)^2 + (z-c)^2}} - \frac{1}{\sqrt{(x-\xi)^2 + (y-\eta)^2 + (z+c)^2}} \right] - \int_{-c}^{+c} dz \frac{\partial}{\partial z} \int_{-b}^b dy \int_{-b}^b d\eta \int_{-a}^a dx \int_w^a d\xi \left[\frac{1}{\sqrt{(x-\xi)^2 + (y-\eta)^2 + (z-c)^2}} - \frac{1}{\sqrt{(x-\xi)^2 + (y-\eta)^2 + (z+c)^2}} \right] \right\}.$$

Taking into account the symmetry properties of the multiple integrals (see Appendix A), one obtains $E_M^{\downarrow\uparrow} = 0$. Thus, the difference $\Delta E_M = E_M^{\downarrow\uparrow} - E_M^{\uparrow\uparrow}$ between the surface magnetostatic energy of the prism in the two-domain configuration and the magnetostatic energy of the same prism in the single-domain configuration is given by

$$\Delta E_M = E_M^{\downarrow\uparrow} - E_M^{\uparrow\uparrow} = -\frac{1}{2} M_s^2 V N_z, \quad (12)$$

i.e., it is just the opposite of the magnetostatic self-energy of the single-domain prism. The explicit expression of ΔE_M , as a function of the reduced thickness $t = b/c$ and of the in-plane aspect ratio $p = a/c$ of the rectangular prism, turns out to be

$$\begin{aligned}
\Delta E_M = E_M^{\downarrow\uparrow} - E_M^{\uparrow\uparrow} \approx & -\frac{\gamma_B}{4\pi} \frac{1}{2} M_s^2 V \left[8 \arctan \left(\frac{pt}{\sqrt{1+p^2+t^2}} \right) \right. \\
& + \frac{2(t^2-1)}{t} \ln \left(\frac{\sqrt{1+p^2+t^2}-p}{\sqrt{1+p^2+t^2}+p} \right) + \frac{2(p^2-1)}{p} \ln \left(\frac{\sqrt{1+p^2+t^2}-t}{\sqrt{1+p^2+t^2}+t} \right) \\
& - 2t \ln \left(\frac{\sqrt{p^2+t^2}-p}{\sqrt{p^2+t^2}+p} \right) - 2p \ln \left(\frac{\sqrt{p^2+t^2}-t}{\sqrt{p^2+t^2}+t} \right) \\
& + \frac{2}{p} \ln \left(\frac{\sqrt{1+t^2}-t}{\sqrt{1+t^2}+t} \right) + \frac{2}{t} \ln \left(\frac{\sqrt{1+p^2}-p}{\sqrt{1+p^2}+p} \right) \\
& + \frac{4(p^3+t^3-2)}{3pt} + \frac{4(p^2+t^2-2)}{3pt} \sqrt{1+p^2+t^2} + \frac{4}{pt} (\sqrt{1+p^2} + \sqrt{1+t^2}) \\
& \left. - \frac{4}{3pt} ((p^2+t^2)^{\frac{3}{2}} + (1+p^2)^{\frac{3}{2}} + (1+t^2)^{\frac{3}{2}}) \right]. \tag{13}
\end{aligned}$$

Clearly, the quantity ΔE_M (see Eq. 12) is always negative: as for the surface contribution to the magnetostatic self-energy, the system would prefer to divide in two domains. In the limit of vanishing thickness, the magnetostatic energy difference ΔE_M approaches 0, since for $t \rightarrow 0$ one has

$$\begin{aligned}
N_z \approx & -4t \ln t \\
& + t \left\{ 4 \ln(2p) - \frac{4}{p} + 2 + \frac{4}{p} \sqrt{1+p^2} + 2 \ln[1 + 2p^2 \sqrt{1+p^2}] \right\} + O(t^2). \tag{14}
\end{aligned}$$

The vanishing of ΔE_M could be expected on general grounds because the number of surface charges tends to 0 as the height of the prism shrinks [18].

A limit to the splitting of the sample in two domains is posed by the full cost of the domain wall energy, which involves other energy terms: exchange interaction and anisotropy. The first term (exchange) is short ranged and favours parallel alignment of neighboring spins:

$$E_{ex} = \frac{A}{M_s^2} \int_V (\nabla \cdot \mathbf{M})^2 dV'. \tag{15}$$

The anisotropy term, assumed to favor the alignment of the magnetization along the z axis, has the form

$$E_{ani} = -\frac{K_1}{M_s^2} \int_V (M^z)^2 dV'. \tag{16}$$

The magnetostatic contribution to the Néel domain wall energy is determined assuming a one-dimensional model of the wall [13], *i.e.*, the magnetization

within the wall ($-w \leq x \leq w$) is a function of x only. The components of the unit magnetization are assumed to be

$$m_x(x) = \frac{w^2}{w^2 + x^2}, \quad m_y(x) = 0, \quad m_z(x) = \frac{x\sqrt{2w^2 + x^2}}{w^2 + x^2}, \quad (17)$$

where w determines the wall width. At the ends of the wall, where the domains begin, one has $m_z(\pm\infty) = \pm 1$. In a thin film, the magnetostatic energy of the volume charges within a Néel wall which occupies the region $-w \leq x \leq w$ can be approximated by [13]

$$E_m = 4\pi M_s^2 b \int_{-\infty}^{\infty} dx [m_x(x)]^2 - 2M_s^2 \int_0^{\infty} dt \frac{1 - e^{-2bt}}{t} \int_{-\infty}^{\infty} dx \int_{-\infty}^{\infty} dx' \cos[(x - x')t] m_x(x)m_x(x'), \quad (18)$$

provided that the domain wall width is much smaller than the lateral dimensions of the sample, $w \ll a \leq c$. In the same approximation, the exchange and the uniaxial anisotropy contributions to the domain wall energy are, respectively

$$E_{ex} = A \int_{-b}^b dy \int_{-\infty}^{\infty} dx \left[\left(\frac{dm_x}{dx} \right)^2 + \left(\frac{dm_z}{dx} \right)^2 \right],$$

$$E_{ani} = K_1 \int_{-b}^b dy \int_{-\infty}^{\infty} dx m_x^2. \quad (19)$$

One finally obtains the following expressions for the magnetostatic, the exchange and the anisotropy contributions

$$\gamma_m = \frac{E_m}{4bc} = \pi^2 M_s^2 w \left[1 - \frac{w}{b} \ln \left(1 + \frac{b}{w} \right) \right], \quad (20)$$

$$\gamma_{ex} = \frac{E_{ex}}{4bc} = \frac{2\pi A}{w} (\sqrt{2} - 1), \quad (21)$$

$$\gamma_{ani} = \frac{E_{ani}}{4bc} = \frac{\pi w}{2} K_1, \quad (22)$$

to the total Néel wall energy $\gamma_N = \gamma_m + \gamma_{ex} + \gamma_{ani}$ per unit wall area ($4bc$). The actual domain wall width is determined by minimizing γ_N with respect

to w , thus leading to the transcendental equation [13]

$$\frac{2A(\sqrt{2}-1)}{\pi M_s^2 w^2} - \frac{K_1}{2\pi M_s^2} - 1 + \frac{2w}{b} \ln\left(1 + \frac{b}{w}\right) - \frac{w}{w+b} = 0. \quad (23)$$

We have solved Eq. (23) using the material parameters of Permalloy (*i.e.*, exchange constant $A = 10^{-6}$ erg/cm, uniaxial anisotropy constant $K_1 = 10^3$ erg/cm³, saturation magnetization $M_s = 800$ emu).

In Fig. 4 (top) we plot the energy density (*i.e.*, the energy per unit wall area $4bc$) versus the in-plane aspect ratio $p = a/c$ of a rectangular prism (larger side $2c = 3 \times 10^{-4}$ cm), for fixed dot thickness ($2b = 3 \times 10^{-6}$ cm). Using the Permalloy material parameters, the calculated energy density turns out to be positive for $p < p_c$ and negative for $p > p_c$, with $p_c = 0.27$. Therefore, an elongated sample ($p < p_c$) prefers to assume a single-domain configuration since the energy density cost of the Néel wall, γ_N , exceeds the gain in surface magnetostatic energy density, $\delta_M = \frac{\Delta E_M}{4bc}$, which is obtained splitting the sample into two domains. Upon increasing the in-plane aspect ratio from the critical value p_c to $p = 1$ (limit of a square dot), there is an increasing gain in the surface magnetostatic energy, and the element prefers to assume a two-domain configuration. In Fig. 4 (bottom) the energy density of a square Permalloy prism (side $2a = 2c = 3 \times 10^{-4}$ cm) is plotted as a function of the reduced thickness $t = b/c$. This means that for a square sample the two-domain state is always preferred, whatever is the thickness.

These theoretical results for rectangular Permalloy prisms appear to account for recent MFM data [3] in a series of *elliptic* patterned Permalloy dots with thickness $2b = 30$ nm. In these samples, one axis of the elliptic elements was kept the same ($2c = 3 \mu\text{m}$) and the other was varied, so that a series of dots with in-plane aspect ratio $p = a/c$ ranging between $p = 0.13$ and $p = 1$ was obtained. Moreover, the interdot distance was kept sufficiently large so as to consider the dots as non interacting. The MFM images clearly showed that elongated dots with $p \leq 0.22$ are in a single-domain configuration, while dots with $p \geq 0.28$ are in a two-domain configuration, in fair agreement with our theoretical result of a critical aspect ratio $p_c = 0.27$. For circular dots, a vortex configuration turned out to be preferred [3].

The shape of the sample is fully determined by the in-plane aspect ratio $p = a/c$ and by the reduced thickness $t = b/c$. In Fig. 5 we plot the critical aspect ratio p_c as a function of t , for Permalloy samples. For not so small thicknesses ($t \sim 0.1$), the sample is always in a two-domain state except for very elongated systems ($p < 0.1$). With decreasing the thickness, the value of p_c increases and for $t < 0.0015$, $p_c > 1$, which means that the system always stays in the single-domain state. This is due to the additional exchange+anisotropy cost of the domain wall, because, as it appears from Eq. (12) and Eq. (14) (see

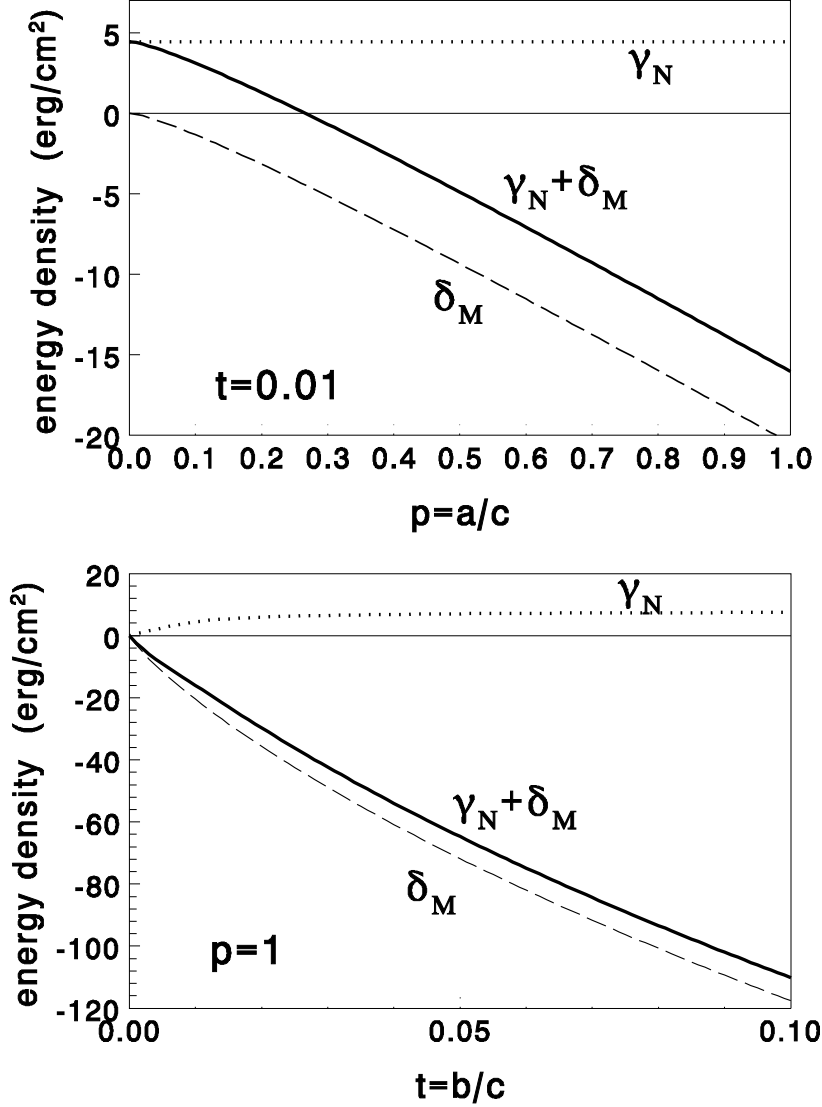


Fig. 4. Top: energy per unit wall area ($4bc$) of a rectangular ferromagnetic Permalloy prism versus the in-plane aspect ratio $p = a/c$ for fixed thickness. The dotted line is the cost in energy density, γ_N , of a Néel wall separating two opposite domains (see Eqs. (20-22)), the dashed line is the gain in magnetostatic energy density, $\delta_M = \frac{\Delta E_M}{4bc}$ (see Eq. (13)), and the full line is the total energy density $\gamma_N + \delta_M$. The single-domain state is energetically favored when $p < p_c = 0.27$, while the two-domain state is preferred for $p_c < p \lesssim 1$. Bottom: energy per unit wall area ($4bc$) of a square ($p = a/c = 1$) ferromagnetic Permalloy prism versus the reduced thickness $t = b/c$. In this case, the two-domain state is always preferred.

also the next Section), the balance of dipolar energy is always in favor of the two-domain state for a square prism ($p = 1$).

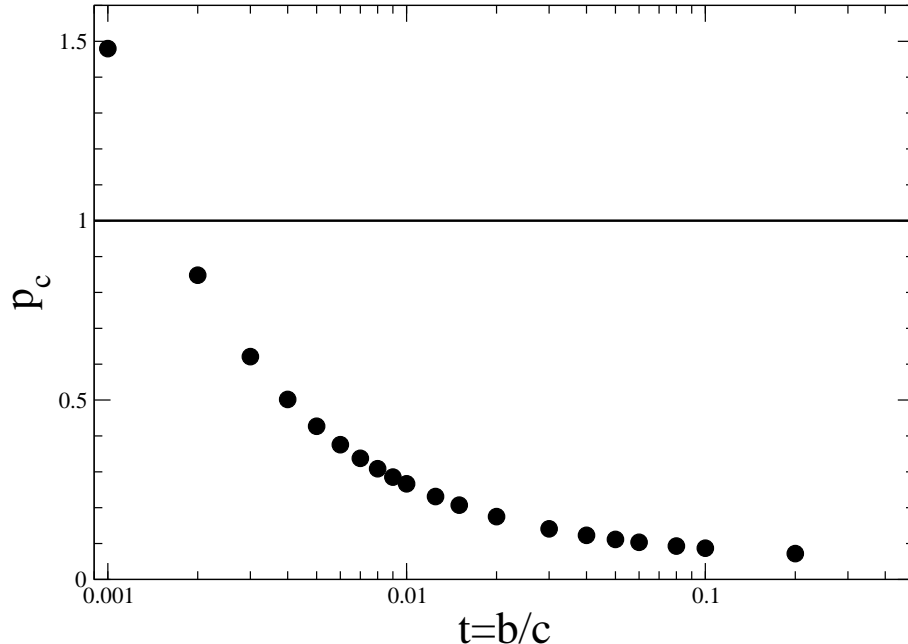


Fig. 5. The critical in-plane aspect ratio p_c as a function of the reduced thickness t , for Permalloy films. A value of p_c larger than 1 (as it is for very small thicknesses) means that the system always stays in a single domain state: this is an effect of the exchange+anisotropy cost of the domain wall.

4 Changing the film thickness: discrete vs continuum approaches

In Section 2 we have shown that a one ML thick magnetic particle does not undergo a splitting from a single-domain to a two-domain state with passing from an elongated to a square sample. In Section 3, within a continuum approach, we have shown that such splitting does exist for a film. Therefore, we should be led to conclude that this transition appears at some critical thickness. In the following we are going to discuss this problem.

First, we observe that the key quantities to be compared are $(E_{1,-1} - E_{1,-1}^{FM})$, $(E_{0,0} - E_{0,0}^{FM})$ in the discrete approach, and $(E_M^{\downarrow\uparrow} - E_M^{\uparrow\uparrow})$, E_m in the continuum approach. The quantities $(E_{1,-1} - E_{1,-1}^{FM})$ and $(E_M^{\downarrow\uparrow} - E_M^{\uparrow\uparrow})$ are negative and mean the gain in dipolar energy when two domains of opposite magnetization are formed. The other quantities, $(E_{0,0} - E_{0,0}^{FM})$ and E_m , are positive and mean the dipolar cost in forming a domain wall. A square-shaped particle can possibly split in two domains only if the dipolar gain is larger than the dipolar cost. In the following we are comparing discrete and continuum expressions of the dipolar gain and of the dipolar cost for a square particle.³

³ An elongated film ($p \ll 1$) is surely in a single domain state. A transition to a two-domain state occurs if and only if a square particle is in a two-domain state.

4.1 The dipolar gain

According to Eq. (12), $\Delta E_M = E_M^{\downarrow\uparrow} - E_M^{\uparrow\uparrow} = -\frac{1}{2}M_s^2VN_z$. The quantity N_z is a complicated expression, but we can confine here to $p = 1$ (square prism) and $t \rightarrow 0$ (vanishing thickness). In these limits, see Eq. (14),

$$\Delta E_M = -\frac{1}{2}M_s^2VN_z \simeq -\frac{1}{2}M_s^2V(-4t \ln t + \bar{c}t), \quad (24)$$

with $\bar{c} \simeq 2.9$. In the ML limit, see Eq. (7), we had

$$E_{1,-1} - E_{1,-1}^{FM} \simeq -1.9\Omega(2L_z). \quad (25)$$

It is worth noting that for both approaches, in the limit of a domain wall width much smaller than the in-plane size of the particle, the dipolar energy gain does not depend on the domain wall width.

If we consider the case of domain wall width much larger than film thickness, $L_{dw} \gg L_y$, the result (25) for the ML can be extended to finite film thickness simply multiplying it by $(2L_y)^2$, because there are $(2L_y)$ stripes magnetized in the \hat{z} direction which interact with the $(2L_y)$ stripes magnetized in the opposite direction, so that

$$E_{1,-1} - E_{1,-1}^{FM} \simeq -1.9\Omega(2L_z)(2L_y)^2 \simeq -\frac{1}{2}M_s^2V(3.8t). \quad (26)$$

Therefore, the discrete approach is directly comparable with the continuum one: the former gives $N_z \approx 3.8t$ and the latter $N_z \approx -4t \ln t + 2.9t$.

4.2 The dipolar cost

According to Eq. (20), the dipolar cost of the Néel wall is

$$E_m = 4bc \pi^2 M_s^2 w \left[1 - \frac{w}{b} \ln \left(1 + \frac{b}{w} \right) \right], \quad (27)$$

where $2w$ is the domain-wall width and $2b$ is the thickness. In the relevant limit $w \gg b$, we get

$$E_m \approx \frac{\pi^2}{4} M_s^2 V t. \quad (28)$$

In the discrete approach for the ML, see Eq. (4) and Fig. 2, we have the corresponding quantity

$$E_{0,0} - E_{0,0}^{FM} \simeq \Omega d_0 (2L_z), \quad (29)$$

with $d_0 \approx 5$. Therefore, for both approaches, the dipolar domain wall energy does not depend on w in the limit $w \ll a$ (or, equivalently, $L_{dw} \ll L_x$).

Extending the discrete approach to a finite thickness, we have to distinguish between interacting spins belonging to the same layer and to different layers. There are $(2L_y)$ planes and $(2L_y)(2L_y - 1)/2$ distinct pairs of planes; within the usual approximation $L_{dw} \gg L_y$, the interaction between different planes within the domain wall does not depend on their distance, so that

$$E_{0,0} - E_{0,0}^{FM} \simeq \Omega(2L_z) \left[d_0(2L_y) + d_1 \frac{(2L_y)(2L_y - 1)}{2} \right] \approx \frac{d_1}{2} M_s^2 V t, \quad (30)$$

where we have retained only the leading term.

In the above expressions, $d_0 \approx 5$, while d_1 represents the interaction energy between different layers within the domain wall. We have numerically checked that $d_1 > 5$, therefore the dipolar energy cost $(d_1/2)M_s^2Vt$ always dominates on the dipolar gain $(-1.9M_s^2Vt)$. On the other hand, in the continuum picture we have a dipolar gain $\Delta E_M = -\frac{1}{2}M_s^2V(-4t \ln t + 2.9t)$ which dominates on the dipolar cost $E_m = (\pi^2/4)M_s^2Vt$ for any thickness t .

To sum up, the continuum approach suggests that a square particle is splitted in two domains for any thickness, while the discrete approach supports the opposite conclusion. However, *extrapolation of the discrete results from the ML to finite thickness is valid only within the limit of thickness much smaller than the domain wall width*. We are therefore led to conclude that a critical thickness $L_y^* \approx L_{dw}$ should exist, such that the transition between single-domain to two-domain state appears at thicknesses $L_y > L_y^*$ only.

5 Conclusions

In Ref. [8] we had considered a single monolayer with planar spins interacting only via dipolar interaction. For a triangular lattice, it was possible to observe a transition from a single-domain to a two-domain to a macrovortex state, when passing from elongated to square (or circular) samples. This phenomenology did not apply to a square lattice, because in that case spins do not like ferromagnetic configurations. The domain wall in the two-domain state was atomically sharp.

In this paper we have studied in detail the transition from a single-domain to a two-domain configuration for a film of general thickness and in the presence of exchange interaction and single ion anisotropy. The presence of the exchange interaction has a twofold effect: it widens the domain wall and, together with the anisotropy, it increases the energetic cost of the domain wall. The first effect (a larger domain wall) is enough to suppress the transition from single domain to two-domain state in a monolayer and in ultrathin films. These results have been obtained within a discrete approach.

For thicker films a continuum, micromagnetic approach is more appropriate. According to it, the energetic balance of the sole dipolar interaction is such that the above transition always occurs on passing from elongated to square samples. When exchange and anisotropy are correctly taken into account in the full energy balance, it is straightforward to realize that the transition may only occur for systems where the anisotropy K_1 is vanishing small, because the exchange A is usually so large that the additional cost in domain wall energy density $\sqrt{AK_1}$ can not be compensated by the gain in dipolar energy density, of order $M_s^2 b$. A material satisfying the condition $\sqrt{AK_1} \ll M_s^2 b$ is Permalloy. For rectangular prisms made of this material, we have therefore determined the critical in-plane aspect ratio p_c as a function of the prism thickness. Fair agreement with existing experimental data on Permalloy particles [3] was obtained.

A final comment concerns the discrete and the continuum approaches. The former has been applied to ultrathin films and has shown that increasing the domain-wall width suppresses the transition. In contrast, the transition is obtained using the latter approach, valid for thicker films. Therefore, these results suggest the existence of some critical thickness d^* above which the transition appears. The discrete formalism suggests that this thickness d^* should be of order of the domain wall width w , but the continuum formalism does not seem to indicate that something “critical” should occur when $b \approx w$. This is the sole issue we have not been able to clarify in full.

Acknowledgements

Work supported by Italian MIUR and CNR (FISR Project “Nanotecnologie per dispositivi di memoria ad altissima densità” and FIRB Project “Microsistemi basati su materiali magnetici innovativi strutturati su scala nanoscopica”).

A Analytical calculation of the multiple integrals

The magnetostatic self-energy of the distributions of surface charges depicted in Fig. 3 can be expressed in terms of the multiple integrals

$$\begin{aligned}
 I^+(w, a, b, k) &= \int_{-b}^b dy \int_{-b}^b d\eta \int_{-a}^{+a} dx \int_w^a d\xi \frac{1}{\sqrt{(x-\xi)^2 + (y-\eta)^2 + k^2}} \\
 I^-(w, a, b, k) &= \int_{-b}^b dy \int_{-b}^b d\eta \int_{-a}^{+a} dx \int_{-a}^{-w} d\xi \frac{1}{\sqrt{(x-\xi)^2 + (y-\eta)^2 + k^2}} \quad (\text{A.1})
 \end{aligned}$$

By symmetry, it immediately turns out that $I^+(w, a, b, k) = I^-(w, a, b, k) = I(w, a, b, k)$ and that $I(w, a, b, -k) = I(w, a, b, k)$. The explicit expression of $I(w, a, b, k)$ is

$$\begin{aligned}
 I(a, b, k) &= \frac{2}{3}(k^2)^{\frac{3}{2}} - \frac{1}{3}(4a^2 + 4b^2 + k^2)^{\frac{3}{2}} + \frac{1}{3}(4a^2 + k^2)^{\frac{3}{2}} + \frac{1}{3}(4b^2 + k^2)^{\frac{3}{2}} \\
 &\quad - \frac{1}{3} \left[((w+a)^2 + k^2)^{\frac{3}{2}} - ((w+a)^2 + 4b^2 + k^2)^{\frac{3}{2}} \right. \\
 &\quad \left. - ((w-a)^2 + k^2)^{\frac{3}{2}} + ((w-a)^2 + 4b^2 + k^2)^{\frac{3}{2}} \right] \\
 &\quad + k^2 \sqrt{4a^2 + 4b^2 + k^2} - k^2 \sqrt{4a^2 + k^2} - k^2 \sqrt{4b^2 + k^2} \\
 &\quad + k^2 \left[\sqrt{(w+a)^2 + k^2} - \sqrt{(w+a)^2 + 4b^2 + k^2} \right. \\
 &\quad \left. - \sqrt{(w-a)^2 + k^2} + \sqrt{(w-a)^2 + 4b^2 + k^2} \right] \\
 &\quad - 8abk \arctan \left(\frac{4ab}{k\sqrt{4a^2 + 4b^2 + k^2}} \right) \\
 &\quad + 4bk \left[(w+a) \arctan \left(\frac{2(w+a)b}{k\sqrt{(w+a)^2 + 4b^2 + k^2}} \right) \right. \\
 &\quad \left. - (w-a) \arctan \left(\frac{2(w-a)b}{k\sqrt{(w-a)^2 + 4b^2 + k^2}} \right) \right] \\
 &\quad + bk^2 \ln \left(\frac{\sqrt{4b^2 + k^2} + 2b}{\sqrt{4b^2 + k^2} - 2b} \right) \\
 &\quad - bk^2 \ln \left(\frac{\sqrt{4a^2 + 4b^2 + k^2} + 2b}{\sqrt{4a^2 + 4b^2 + k^2} - 2b} \right) \\
 &\quad + 4a^2b \ln \left(\frac{\sqrt{4a^2 + 4b^2 + k^2} + 2b}{\sqrt{4a^2 + 4b^2 + k^2} - 2b} \right)
 \end{aligned}$$

$$\begin{aligned}
& + 2ak^2 \ln \left(\sqrt{4a^2 + k^2} + 2a \right) \\
& + k^2 \left[- (w + a) \ln \left(\sqrt{(w + a)^2 + k^2} - (w + a) \right) \right. \\
& \left. + (w - a) \ln \left(\sqrt{(w - a)^2 + k^2} - (w - a) \right) \right] \\
& - 2ak^2 \ln \left(\sqrt{4a^2 + 4b^2 + k^2} + 2a \right) \\
& + k^2 \left[(w + a) \ln \left(\sqrt{(w + a)^2 + 4b^2 + k^2} - (w + a) \right) \right. \\
& \left. - (w - a) \ln \left(\sqrt{(w - a)^2 + 4b^2 + k^2} - (w - a) \right) \right] \\
& - 8ab^2 \ln \left(\sqrt{4a^2 + 4b^2 + k^2} - 2a \right) \\
& + 4b^2 \left[(w + a) \ln \left(\sqrt{(w + a)^2 + 4b^2 + k^2} - (w + a) \right) \right. \\
& \left. - (w - a) \ln \left(\sqrt{(w - a)^2 + 4b^2 + k^2} - (w - a) \right) \right] \\
& + b \left[(k^2 - (w + a)^2) \ln \left(\frac{\sqrt{(w + a)^2 + 4b^2 + k^2} + 2b}{\sqrt{(w + a)^2 + 4b^2 + k^2} - 2b} \right) \right. \\
& \left. - (k^2 - (w - a)^2) \ln \left(\frac{\sqrt{(w - a)^2 + 4b^2 + k^2} + 2b}{\sqrt{(w - a)^2 + 4b^2 + k^2} - 2b} \right) \right] \\
& - k^2 \left[(w + a) \ln \left(\frac{\sqrt{(w + a)^2 + k^2} + (w + a)}{\sqrt{(w + a)^2 + k^2} - (w + a)} \right) \right. \\
& \left. + (w - a) \ln \left(\frac{\sqrt{(w - a)^2 + k^2} - (w - a)}{\sqrt{(w - a)^2 + k^2} + (w - a)} \right) \right] \\
& + k^2 \left[(w + a) \ln \left(\frac{\sqrt{(w + a)^2 + 4b^2 + k^2} + (w + a)}{\sqrt{(w + a)^2 + 4b^2 + k^2} - (w + a)} \right) \right. \\
& \left. + (w - a) \ln \left(\frac{\sqrt{(w - a)^2 + 4b^2 + k^2} - (w - a)}{\sqrt{(w - a)^2 + 4b^2 + k^2} + (w - a)} \right) \right] \tag{A.2}
\end{aligned}$$

Taking the limit $w \rightarrow 0$ in the terms in square parentheses on the r.h.s., one obtains

$$I(0, a, b, k) = \frac{2}{3}(k^2)^{\frac{3}{2}} - \frac{1}{3}(4a^2 + 4b^2 + k^2)^{\frac{3}{2}}$$

$$\begin{aligned}
& + \frac{1}{3}(4a^2 + k^2)^{\frac{3}{2}} + \frac{1}{3}(4b^2 + k^2)^{\frac{3}{2}} \\
& + k^2 \sqrt{4a^2 + 4b^2 + k^2} \\
& - k^2 \sqrt{4a^2 + k^2} - k^2 \sqrt{4b^2 + k^2} \\
& - 8abk \arctan \left(\frac{4ab}{k\sqrt{4a^2 + 4b^2 + k^2}} \right) \\
& + bk^2 \ln \left(\frac{\sqrt{4b^2 + k^2} + 2b}{\sqrt{4b^2 + k^2} - 2b} \right) \\
& - bk^2 \ln \left(\frac{\sqrt{4a^2 + 4b^2 + k^2} + 2b}{\sqrt{4a^2 + 4b^2 + k^2} - 2b} \right) \\
& + 4a^2b \ln \left(\frac{\sqrt{4a^2 + 4b^2 + k^2} + 2b}{\sqrt{4a^2 + 4b^2 + k^2} - 2b} \right) \\
& + ak^2 \ln \left(\frac{\sqrt{4a^2 + k^2} + 2a}{\sqrt{4a^2 + k^2} - 2a} \right) \\
& - ak^2 \ln \left(\frac{\sqrt{4a^2 + 4b^2 + k^2} + 2a}{\sqrt{4a^2 + 4b^2 + k^2} - 2a} \right) \\
& + 4ab^2 \ln \left(\frac{\sqrt{4a^2 + 4b^2 + k^2} + 2a}{\sqrt{4a^2 + 4b^2 + k^2} - 2a} \right)
\end{aligned} \tag{A.3}$$

Dropping the a, b arguments for brevity's sake, and taking into account the symmetry properties of the multiple integrals, the magnetostatic self-energy for the one-domain configuration (see Fig. 3, top) is expressed as

$$\begin{aligned}
E_M^{\uparrow\uparrow} &= \frac{\gamma_B}{4\pi} \frac{1}{2} M_s^2 \left[I^-(0, 0) - I^-(0, -2c) + I^+(0, 0) - I^+(0, -2c) \right. \\
& \left. - I^-(0, 2c) + I^-(0, 0) - I^+(0, 2c) + I^+(0, 0) \right] \\
&= \frac{\gamma_B}{4\pi} M_s^2 2 \left[I(0, 0) - I(0, 2c) \right]
\end{aligned} \tag{A.4}$$

Upon substituting the explicit expression of the multiple integral (A.3) in the equation (A.4), it is immediate to recover Aharoni's formula for the demagnetizing factor of the uniform and homogeneous ferromagnetic rectangular prism (Eq. 1 of Aharoni's paper) [10].

For the two-domain configuration (see Fig. 3, bottom), the contribution of the surface charges to the magnetostatic energy is found to be

$$\begin{aligned}
E_M^{\downarrow\uparrow} &= \frac{\gamma_B}{4\pi} \frac{1}{2} M_s^2 \left[I^-(w, 0) - I^-(w, -2c) - I^+(w, 0) + I^+(w, -2c) \right. \\
& \left. - I^-(w, 2c) + I^-(w, 0) + I^+(w, 2c) - I^+(w, 0) \right]
\end{aligned} \tag{A.5}$$

so that, taking into account the symmetry properties of the integrals, $E_M^{\downarrow\uparrow}$

is found to vanish. In conclusion, the magnetostatic energy difference ΔE_M turns out to be just the opposite of the magnetostatic self-energy of the single-domain prism. Its explicit expression is given in the main text, Eq. (13), in terms of the in-plane aspect ratio, $p = a/c$, and of the reduced thickness, $t = b/c$, of the rectangular prism.

References

- [1] C. Stamm, F. Marty, A. Vaterlaus, V. Weich, S. Egger, U. Maier, U. Ramsperger, F. Fuhrmann, D. Pescia, *Science* **282**, 449 (1998).
- [2] G. A. Prinz, *Science* **282**, 1660 (1998).
- [3] A. Imre, G. Csaba, L. Ji, A. Orlov, G. H. Bernstein, W. Porod, *Science* **311**, 205 (2006).
- [4] A. N. Broers, *Phil. Trans. R. Soc. A* **353**, 291 (1995).
- [5] R. P. Cowburn, *J. Phys. D: Appl. Phys.* **33**, R1-R16 (2000).
- [6] X. Zhu and P. Grutter, *IEEE Trans. on Magn.* **39**, 3420 (2003).
- [7] P. Politi and M.G. Pini, *Eur. Phys. J. B* **2**, 475 (1998).
- [8] P. Politi, M. G. Pini, and R. L. Stamps, *Phys. Rev. B* **73**, 020405(R) (2006).
- [9] V. M. Rozenbaum, V. M. Ogenko, and A. A. Chuiko, *Usp. Fiz. Nauk.* **161**, 79 (1991) [*Sov. Phys. Usp.* **34**, 883 (1992)].
- [10] A. Aharoni, *J. Appl. Phys.* **83**, 3432 (1998).
- [11] P.-O. Jubert and R. Allenspach, *Phys. Rev. B* **70**, 144402 (2004).
- [12] A. Aharoni, *J. Appl. Phys.* **37**, 3271 (1966).
- [13] A. Aharoni, *Introduction to the Theory of Ferromagnetism*, (Clarendon Press, Oxford, 1996).
- [14] O. Portmann, M. Buess, A. Vindigni, A. Vaterlaus, D. Pescia, C.H. Back, *Thin Sol. Films* **505**, 2 (2006).
- [15] P. Politi, *Comments Cond. Matter Phys.* **18**, 191 (1998).
- [16] A. B. Kashuba and V. L. Pokrovsky, *Phys. Rev. B* **48**, 10335 (1993).
- [17] A. Aharoni, *IEEE Transact. on Magnetism* **27**, 3539 (1991).
- [18] J. Harris and D. Awschalom, *Thin films squeeze out domains*, in *Physics World*, January 1999, p.19.